

# Structural formation of poly(ethylene terephthalate) during the induction period of crystallization: 1. Ordered structure appearing before crystal nucleation

M. Imai, K. Mori and T. Mizukami

Research Center, Toyobo Co. Ltd, Otsu, Shiga 520-02, Japan

and K. Kaji\* and T. Kanaya

Institute for Chemical Research, Kyoto University, Uji, Kyoto-fu 611, Japan

(Received 8 August 1991; revised 26 November 1991; accepted 27 December 1991)

A new finding is reported concerning some structural change in the amorphous state of the polymer which occurs during the so-called induction period before the start of crystallization. Annealing of poly(ethylene terephthalate) (PET) at 115°C, or 40°C above the glass transition temperature,  $T_g$ , has been investigated by small-angle X-ray scattering (SAXS) and wide-angle X-ray scattering (WAXS) techniques. At a very early stage of the induction period the SAXS intensity starts to increase in the range of  $Q = 0.02\text{--}0.04 \text{ \AA}^{-1}$ , where  $Q$  is the length of the scattering vector ( $Q = 4\pi \sin \theta/\lambda$ ), and continues to increase until the beginning of crystallization. Corresponding to the initiation of crystallization, another strong peak, caused by the usual long-period structure, appears in the vicinity of  $Q = 0.05 \text{ \AA}^{-1}$ . It is confirmed from the WAXS measurements that no local ordering takes place during the induction period. To clarify the crystallization process, distance distribution analysis is also carried out.

(Keywords: structural formation; crystallization; induction period; small-angle X-ray scattering; wide-angle X-ray scattering; distance distribution analysis; poly(ethylene terephthalate))

## INTRODUCTION

Extensive studies have been performed on the morphology of crystalline polymers obtained by annealing the glass or by cooling the melt<sup>1-8</sup>. However, most of these studies have been limited to the observation of crystal growth processes and little information exists about how nucleation proceeds from the disordered amorphous state.

Geil<sup>9</sup> has reported an amorphous structure having nodules of about 100 Å in diameter based on the observation of low temperature annealed poly(ethylene terephthalate) (PET) samples by transmission electron microscopy. Herglotz<sup>10</sup> has found that crystalline PET films annealed from the glass have a supermolecular structure with a size of about 1000 Å. These experimental results indicate that the long-range structure is formed during the annealing processes of PET. However, the existence of the long-range ordered structure before crystallization in the initial stage of annealing and the relationship between this structure and crystallization processes have not yet been clarified.

The purpose of the present study is to investigate in detail the structural formation in PET when annealed from the glassy state, using X-ray scattering techniques. We focus particularly on clarifying the ordering processes in the very early stage of annealing. PET is a suitable

substance for investigating the structural formation by annealing because it has a high glass transition temperature (75°C) and a very slow crystallization rate. The X-ray scattering measurements were carried out in a very wide  $Q$  range of  $0.01\text{--}4 \text{ \AA}^{-1}$  in order to obtain information about ordering processes for both long-range and local structure. For a more detailed analysis we performed distance distribution analysis in the distance range of 0–800 Å by the inverse Fourier transform of the observed X-ray scattering curves. The distance distribution function also provides useful information concerning the long-range and local structure in the amorphous and semicrystalline states of polymers.

## EXPERIMENTAL

### Sample preparation

The PET used for this study had a number-average molecular weight,  $M_n$ , of 25 000 and a polydispersity,  $M_w/M_n$ , of 2.5 and was supplied by Toyobo Co. Ltd. This polymer contained only 30 ppm phosphor and 30 ppm germanium as additives, so that the scattering from these impurities was negligible.

In order to obtain amorphous samples, the PET was melted at 290°C for 2 min and immediately quenched in ice-water. The density of the melt-quenched sample was  $1.333 (\pm 0.002) \text{ g cm}^{-3}$ , which agrees with the value reported for amorphous PET<sup>11-13</sup>. The annealing of the melt-quenched samples was performed at 115°C, or

\*To whom correspondence should be addressed

40°C above the glass transition temperature, for 10 s, 1, 5 and 20 min in an oil bath. All the samples were then quenched in ice-water. The densities of the samples were measured in a density gradient column with a mixture of *n*-hexane and carbon tetrachloride.

#### X-ray scattering measurements

The melt-quenched and the annealed samples were investigated using small-angle and wide-angle X-ray scattering (SAXS and WAXS) methods. The SAXS measurements were performed on the 6 m point focusing SAXS camera at the High-Intensity X-ray Laboratory of Kyoto University<sup>14</sup>. This camera utilizes Ni-filtered CuK $\alpha$  radiation from a 3.5 kW rotating-anode X-ray generator (RU-1000C3, Rigaku Denki Co. Ltd, Japan), Franks-type double-focusing point collimator, and two-dimensional position-sensitive proportional counter. The scattering intensity after subtraction of the background was circularly averaged since the scattering patterns were azimuthally isotropic. The measurements were carried out for two  $Q$  ranges of 0.01–0.05 Å<sup>-1</sup> and 0.04–0.2 Å<sup>-1</sup>. The observed scattering curves in these two  $Q$  ranges were superposed by vertical shift so that they would coincide in the overlapped  $Q$ -range.

The WAXS measurements were performed using Ni-filtered CuK $\alpha$  X-ray generated from a 4.0 kW Rigaku RAD-rA and a diffractometer with a pinhole collimation system and a scintillation counter. The scattering intensity was measured in the range of 3–70° in the scattering angle  $2\theta$ . The data obtained were corrected for background scattering, polarization, absorption and incoherent scattering.

#### Distance distribution analysis

The spatial correlation function for the system is the average of the product of two electron density fluctuations at a distance  $R$ , defined as:

$$\gamma(R) = \langle \eta(R_1)\eta(R_2) \rangle \quad (1)$$

where  $R = R_1 - R_2$ ,  $\eta(R) = \rho(R) - \bar{\rho}$ ,  $\rho(R)$  being the electron density at  $R$ , and  $\bar{\rho}$  the average in the whole system. Further, the distance distribution function, defined as:

$$P(R) = 4\pi R^2 \gamma(R) \quad (2)$$

is proportional to the number of pairs of difference electrons separated by the distance  $R$ . The  $P(R)$  function is given by the inverse Fourier transform of the scattering intensity  $I(Q)$ :

$$P(R) = (2/\pi) \int I(Q) R Q \sin(RQ) dQ \quad (3)$$

First we calculated the  $P(R)$  functions for a wide  $R$  range of 0–600 Å in order to observe the characteristics for the  $P(R)$  functions of the whole distance range. For this purpose, we obtained the scattering profiles for a wide  $Q$  range of 0.01–4 Å<sup>-1</sup> by combining the SAXS and WAXS curves so that both curves would coincide in the overlapped  $Q$  range. To calculate  $P(R)$  from the observed scattering intensity,  $I(Q)$ , using equation (1), it is necessary to extrapolate the observed scattering curves from  $Q = 0$  to  $Q = \infty$ . For the extrapolation to  $Q = 0$ , we used the Guinier approximation and for the extrapolation to  $Q = \infty$ , we applied the  $Q^{-n}$  law until  $Q = 10 \text{ Å}^{-1}$  and a damping factor  $\exp(-aQ^2)$  with

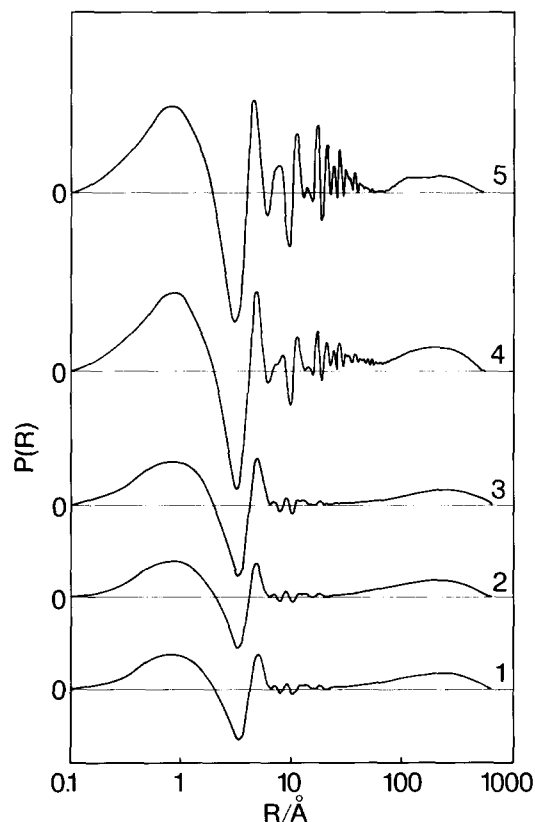


Figure 1 Whole  $P(R)$  functions in the range of 0–600 Å as a function of annealing time at 115°C. 1, Melt-quenched sample; annealing time for other samples: 2, 10 s; 3, 1 min; 4, 5 min; 5, 20 min

$a = 0.01 \text{ Å}^2$ . Figure 1 shows the  $P(R)$  functions in the range of 0–600 Å as a function of annealing time. These  $P(R)$  functions in the middle distance range (10–50 Å), corresponding to crystallite size, show a complex shape because in this region the correlation peaks arising from the long-range and short-range order are overlapped. In order to avoid this overlapping influence, we calculated the  $P(R)$  functions from the SAXS and WAXS profiles separately, and checked the consistency of these  $P(R)$  functions with the whole range functions. We will discuss the profiles of  $P(R)$  functions using these separated profiles.

#### Crystallization isotherm

The crystallization isotherm  $\phi(t)$  was calculated from the following equation:

$$\phi(t) = \frac{\int_0^t (dH_c/dt) dt}{\int_0^\infty (dH_c/dt) dt} \quad (4)$$

where  $dH_c/dt$  is the rate of evolution of heat measured by differential scanning calorimetry (d.s.c.).

## RESULTS AND DISCUSSION

#### Crystallization isotherm

The glass transition temperature and the melting temperature of the samples are 75°C and 250°C, respectively. Figure 2 shows the crystallization isotherm  $\phi(t)$  and the observed densities as a function of annealing time  $t$  at 115°C. Both curves in Figure 2 exhibit similar

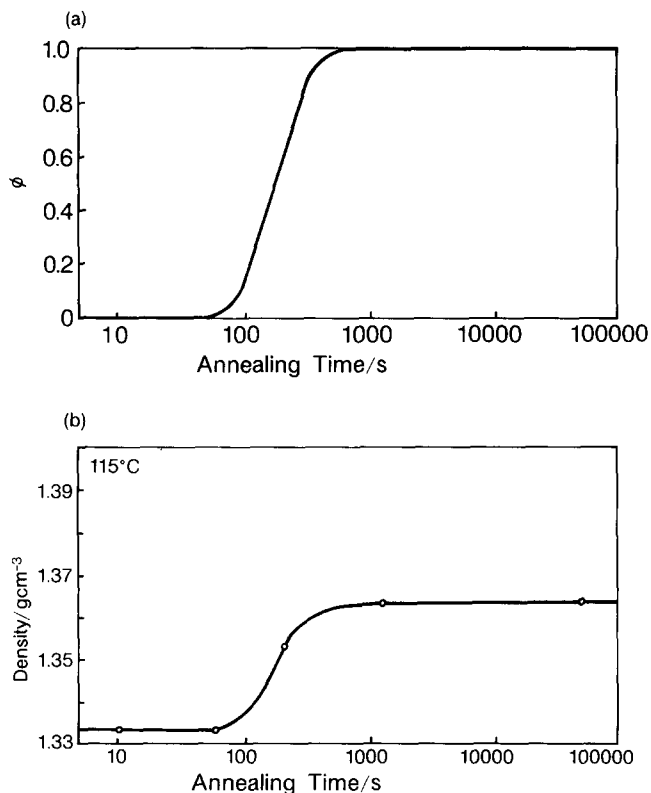


**Figure 2** Annealing time dependence of crystallization isotherm (a) and the macroscopic density (b) for PET. Annealing temperature is 115°C

behaviour and have a sigmoidal shape, typical of polymer crystallization behaviour. During the first 1 min, these values do not change from the initial values, indicating the so-called induction period. During the induction period the sample maintains a constant density of 1.333 g cm<sup>-3</sup>, the same value as that of amorphous PET. After 100 s of annealing, the isotherm and the density increase rapidly, suggesting the initiation of crystallization. As will be confirmed later from WAXS measurements, these abrupt changes actually correspond to crystallization. Therefore, the annealing process after 100 s is termed the crystallization stage. After 20 min the density reaches an equilibrium value of 1.363 g cm<sup>-3</sup>, which corresponds to a degree of crystallinity in volume fraction  $X_c$  of 24.6% according to the relation:

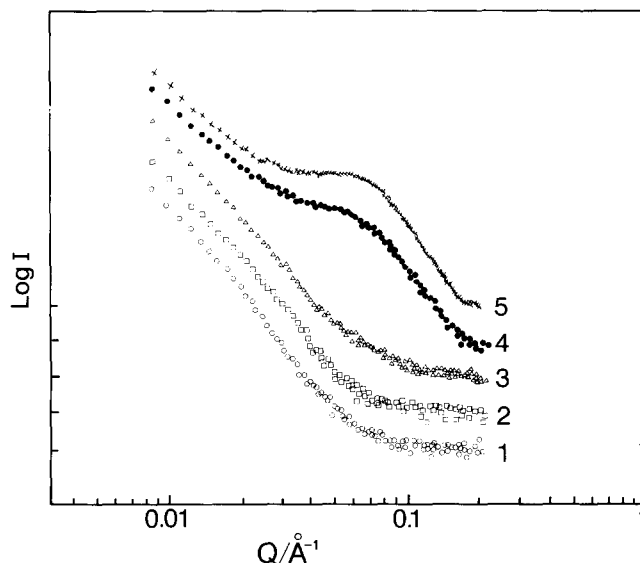
$$X_c = (\rho - \rho_a) / (\rho_c - \rho_a) \quad (5)$$

where  $\rho$ ,  $\rho_c$  and  $\rho_a$  represent the densities of the sample, the crystalline part (1.455 g cm<sup>-3</sup>), and the amorphous part (1.333 g cm<sup>-3</sup>), respectively<sup>13</sup>.

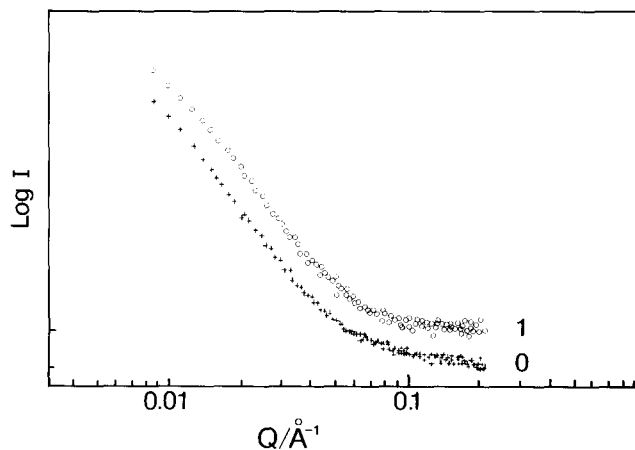
*Long-range structure during annealing*

Figure 3 shows time-resolved SAXS profiles of PET at 115°C; the relative intensity at a given time is plotted as a function of  $Q$  in double logarithmic scale. For convenience each curve is shifted along the intensity axis. The scattering profiles of samples annealed for 10 s and 1 min correspond to the induction period, and those for 5 and 20 min to the crystallization stage. Both features are evident in the time evolution of the SAXS profiles: one is the existence of strong scattering in a very small angle range and the other is the increase of scattering intensity at around  $Q = 0.03 \text{ \AA}^{-1}$  during the induction period.

Regarding the first feature, this very small angle scattering is observed for every sample, even the melt-quenched sample. This strong scattering is not due to the structure produced through the quenching process because it is also observed for the melt sample, as seen from Figure 4. Therefore, this very small angle scattering is a consequence of the heterogeneity in the amorphous state. We estimated the size of this heterogeneity from distance distribution analysis. Figure 5 shows the distance



**Figure 3** SAXS profiles of PET during annealing process. Curve numbers as in Figure 1



**Figure 4** SAXS profiles of PET: 0, melt sample; 1, melt-quenched film

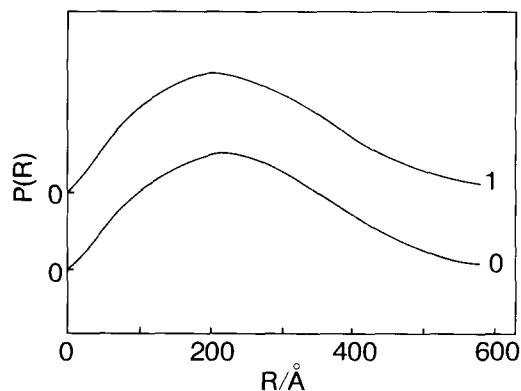


**Figure 5**  $P(R)$  functions of PET: 0, melt sample; 1, melt-quenched film

distribution functions,  $P(R)$ , for the melt and melt-quenched state obtained from *Figure 4*. Both  $P(R)$  functions have a broad peak having a maximum at about 250 Å. The so-called correlation length is defined as:

$$l_c = 2 \int_0^{\infty} \gamma(R) dR \quad (6)$$

where  $\gamma(R)$  is the correlation function normalized by  $\gamma(0) = 1$ . The calculated correlation length according to equation (6) is almost in agreement with the peak position of the  $P(R)$  function. For convenience, we call the peak position in the  $P(R)$  function the correlation length. This peak position depends somewhat on the functions used for extrapolation to  $Q = 0$ . For example, a Lorentzian provides a correlation length of about 300 Å. Here we adopt the value of 250 Å obtained by the Guinier approximation as a measure of correlation length. This correlation length indicates the existence of a structure of about 250 Å in size in the amorphous state. A similar strong intensity in the very small angle X-ray scattering range from amorphous polymers has been reported<sup>15,16</sup>. However, the cause of this is not yet clear, although a small amount of foreign particles existing in the polymer matrix<sup>15</sup> and the polydispersity<sup>16</sup> of a sample were proposed as possible factors. For example, Wendorff and Fischer<sup>15</sup> attributed this to additives or foreign particles, but in our case the PET samples contain only 30 ppm phosphor and 30 ppm germanium as additives. The contribution of these additives to the total scattering intensity is calculated to be less than 1% from their atomic scattering factors. On the other hand, there

are some studies on the long-range structure existing in the amorphous or semicrystalline state. Debye and Bueche<sup>17</sup> have found a correlation length of 2800 Å in amorphous poly(methyl methacrylate) by light scattering measurement. At present, we cannot conclude the origin of this very small angle X-ray scattering, but we consider that it may arise from the density fluctuation of PET itself in the amorphous state because we found that this length depends on the molecular weight of the sample used<sup>18</sup>.

We now discuss the change of the SAXS profiles during the induction period. From *Figure 3* it can be seen that after annealing for 10 s the scattering intensity around  $Q = 0.03 \text{ \AA}^{-1}$  starts to increase. It is surprising that ordering in the long-range scale (about 200 Å) initiates at a very early stage of the induction period though the macroscopic density of the system still does not change. This increase of the intensity is also observed when the sample is annealed for 1 min. After the induction period, a new scattering peak corresponding to a usual long period due to the regular alternation of crystalline and amorphous regions appears at around  $Q = 0.05 \text{ \AA}^{-1}$  and increases in intensity with annealing time. The strong peak of the long period conceals the weak shoulder at around  $Q = 0.03 \text{ \AA}^{-1}$ . In order to analyse the change of the scattering profiles during the induction period in more detail, we subtracted the intensity of the melt-quenched sample from those of the annealed samples. The difference scattering intensities of the samples for the induction period and for the crystallization stage are shown in *Figures 6a* and *b*, respectively. In *Figure 6a* a single scattering maximum is observed at

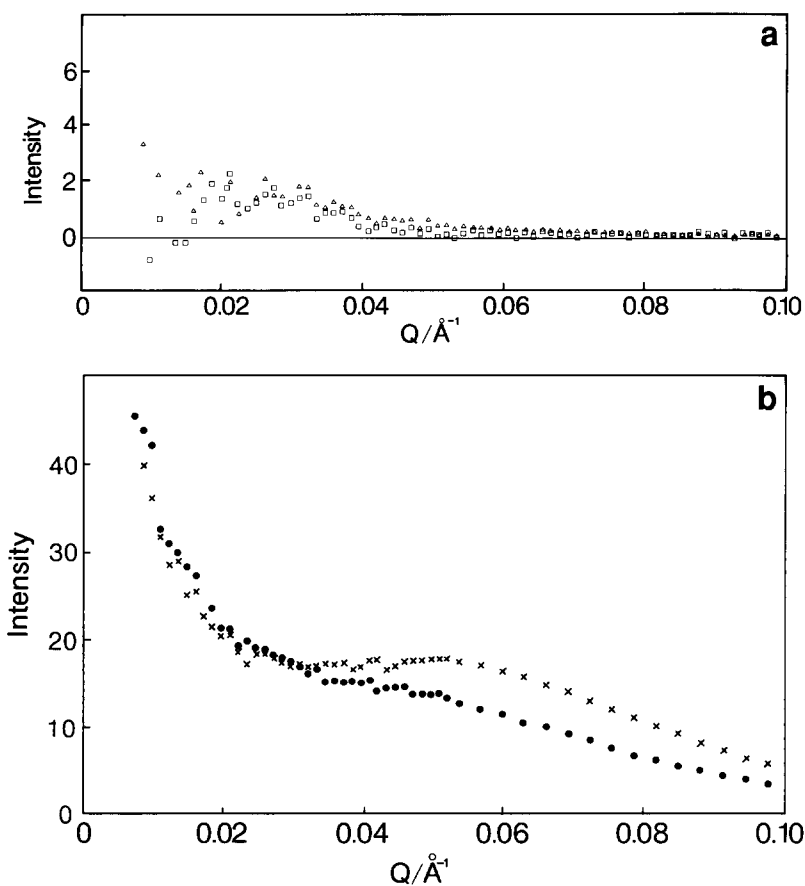


**Figure 6** Difference scattering profiles of the annealed PET films obtained after subtraction of the scattering intensity from the melt-quenched film. (a) Induction period: □, 10 s; △, 1 min. (b) Crystallization stage: ●, 5 min; ×, 20 min

around  $Q = 0.03 \text{ \AA}^{-1}$  for 10 s annealing. This peak suggests that some ordered structure is already formed in the initial stage of the induction period. For 1 min annealing, the intensity also increases in a lower  $Q$  region below  $0.02 \text{ \AA}^{-1}$ , so that the scattering maximum is not observed. After the induction period, the scattering peak at around  $Q = 0.05 \text{ \AA}^{-1}$ , due to the long-period structure, appears and increases in intensity with annealing time as shown in Figure 6b. It should also be noted that the additional intensity in the  $Q$  range below about  $0.02 \text{ \AA}^{-1}$ , as described above, increases remarkably after the initiation of crystallization. This excess scattering indicates the formation of another large-scale structure, which is different from the structure with a size of  $250 \text{ \AA}$  observed in the melt-quenched sample because this is the intensity after subtraction of scattering intensity from the melt-quenched sample. We consider that this may correspond to the supermolecular structure with a size of about  $1000 \text{ \AA}$  reported by Herglotz<sup>10</sup>.

To clarify the crystallization process we calculated the  $P(R)$  functions. Figure 7 shows the  $P(R)$  functions in the range of  $0\text{--}800 \text{ \AA}$  as a function of annealing time. We first notice that the  $P(R)$  of every sample has a broad correlation peak with a maximum at about  $250 \text{ \AA}$ ; this correlation peak was discussed earlier. In the  $P(R)$  functions, however, the correlation peaks corresponding to the scattering peaks at around  $Q = 0.03 \text{ \AA}^{-1}$  which were observed during the induction period are not seen. This is because the scattering intensity of such peaks is very weak compared with the other peaks, so that they may be considered to have disappeared by the inverse Fourier transform where artificial procedures such as extrapolation and damping were applied. In the crystallization stage, however, it deforms remarkably in the range of  $0\text{--}300 \text{ \AA}$ . Thus new correlation peaks appear at  $40 \text{ \AA}$  and  $120 \text{ \AA}$ ; these peaks are attributed to the average crystallite size and the long period, respectively. These peaks increase in intensity with annealing time and in the sample annealed for 20 min a higher order correlation peak appears at about  $230 \text{ \AA}$ , which may be the second peak of the long period.

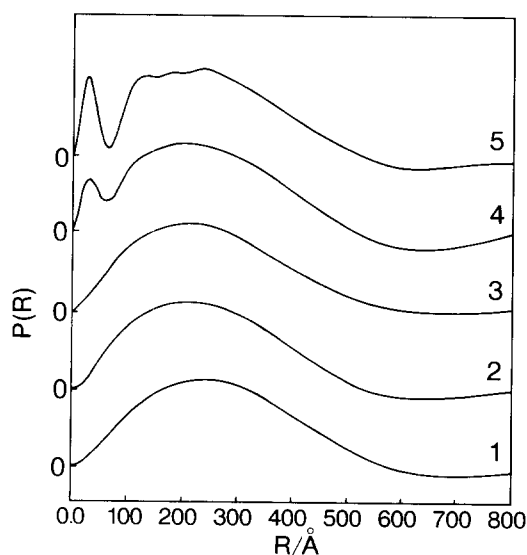


Figure 7  $P(R)$  functions calculated from SAXS profiles in the range of  $0\text{--}800 \text{ \AA}$  as a function of annealing time at  $115^\circ\text{C}$ . Curve numbers as in Figure 1

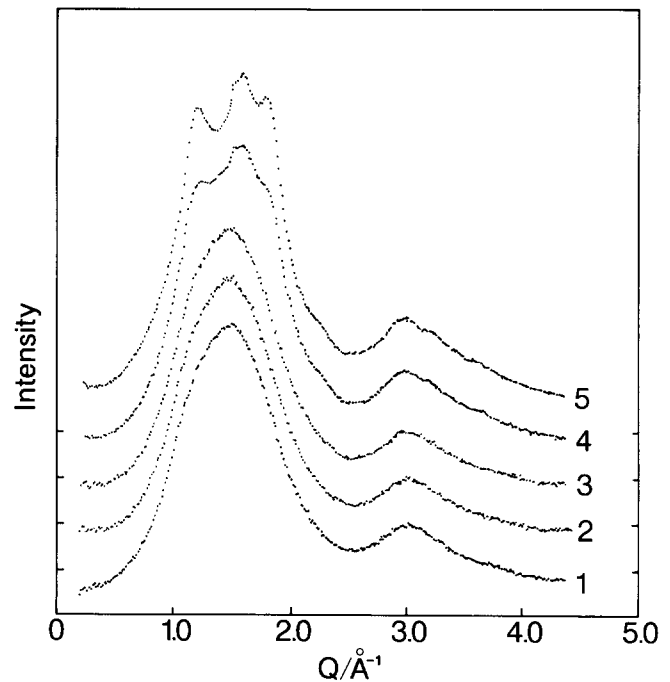


Figure 8 WAXS profiles for PET during annealing. Curve numbers as in Figure 1

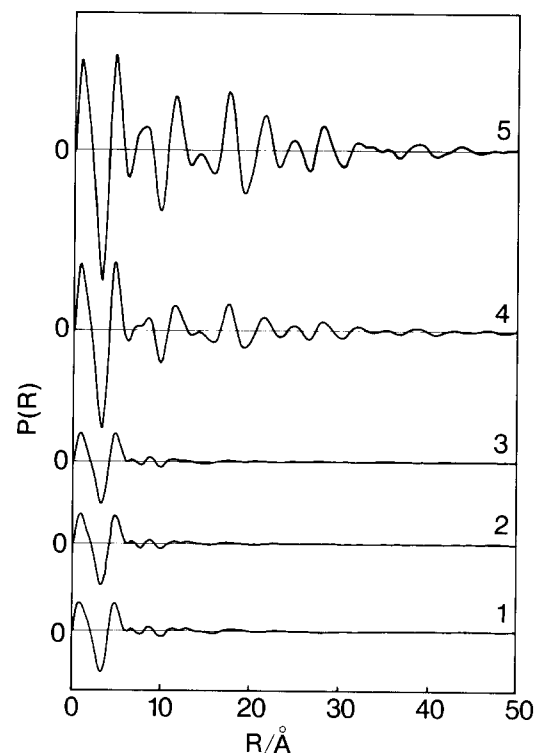


Figure 9  $P(R)$  functions calculated from WAXS profiles in the range of  $0\text{--}50 \text{ \AA}$  as a function of annealing time at  $115^\circ\text{C}$ . Curve numbers as in Figure 1

#### Short-range structure during annealing

In the previous section we have shown that some long-range ordered structure having a size of about  $200 \text{ \AA}$  is formed during the induction period before the long-spacing structure appears. In order to confirm that crystallization does not occur in the induction period, we have made time evolution measurements of WAXS. Figure 8 shows the annealing time dependence of WAXS

profiles at 115°C. Up to 1 min annealing time the diffraction profile does not change from the amorphous pattern of the melt-quenched sample. After 5 min, however, the WAXS pattern shows that the sample starts to crystallize; the strongest halo begins to split into several diffraction peaks, which become sharper with annealing time. These results show that the local ordering or crystallization occurs only after the end of the induction period, i.e. only after the sudden increase of the macroscopic density and the thermogram of the sample in Figure 2.

Figure 9 shows the  $P(R)$  functions in the range of 0–50 Å calculated from the WAXS profiles during annealing. The  $P(R)$  function for the melt-quenched amorphous PET has prominent correlation peaks at 2.5 and 5.0 Å and weak peaks at 7, 9, 12, 14 and 18 Å. The first peak at 2.5 Å is attributed to the intramolecular distance and the second peak at 5.0 Å to the nearest neighbour intermolecular distance<sup>19</sup>.

The  $P(R)$  function for the melt-quenched sample damps rapidly with distance when  $R > 5$  Å. This damping behaviour indicates that the local structure of the melt-quenched PET is random or disordered. The profile of  $P(R)$  in this range remains unchanged up to 1 min annealing time. After 5 min it suddenly changes: the peaks become sharper and more intense, and many additional peaks appear in the range of 20–40 Å. These results confirm that crystallization initiates after 5 min annealing time.

#### Structure formation during the induction period

When the glassy PET is annealed at 115°C, or 40°C above the glass transition temperature, a long-range ordered structure with a size of 200 Å is formed during the induction period.

According to the nucleation growth theory<sup>20</sup> of crystallization, the induction period is considered as the time needed to reach the steady state of nucleation growth directly from the amorphous state, where nuclei are assumed to have a crystal-like structure. In the present study, however, we obtained the following three results for the induction period: (1) the macroscopic density of the sample remains unchanged from that of the amorphous state; (2) no exothermic peak caused by crystallization is observed in the d.s.c. curve; and (3) no local ordering of the chain segments is seen in the distance distribution curve. These observations suggest that no crystallization takes place in the induction period. It is only after the end of the induction period that the macroscopic density begins to increase and crystallization or local ordering starts, probably as a result of the formation of crystal nuclei. All of these experimental facts

strongly support the theory that long-range ordering takes place before the formation of crystal nuclei. The long-range density fluctuation formed in the induction period is considered to be the precursor of the crystal nuclei. This density fluctuation is highly regular and the size of fluctuation is larger than the so-called long period. We consider that the crystal nuclei may be formed in the dense domains of this density fluctuation only after the size of the fluctuation grows to a certain value; the time for this to take place may be the induction period. We will discuss structure formation before crystallization in more detail in a subsequent paper.

#### ACKNOWLEDGEMENTS

We are indebted to the Committee of the High Intensity X-ray Laboratory of Kyoto University for the small-angle X-ray scattering system. We would also like to express our sincere thanks to Dr H. Hayashi and Dr S. Suehiro for experimental support and helpful discussions.

#### REFERENCES

- 1 Sedláček, B. (Ed.) 'Morphology of Polymers', Walter de Gruyter, Berlin, 1986
- 2 Geil, P. H. *Ind. Eng. Chem., Prod. Res. Dev.* 1975, **14**, 59
- 3 Peterlin, A. *J. Polym. Sci.* 1965, **C9**, 61
- 4 Yeh, G. S. Y. and Geil, P. H. *J. Macromol. Sci. Phys.* 1967, **B1**, 235
- 5 Groeninckx, G., Reynaers, H., Berghmans, H. and Smets, G. *J. Polym. Sci., Polym. Phys. Edn* 1980, **18**, 1311
- 6 Groeninckx, G. and Reynaers, H. *J. Polym. Sci., Polym. Phys. Edn* 1980, **18**, 1325
- 7 Gilmer, J. W., Wiswe, D., Zachmann, H. G., Kulger, J. and Fischer, E. W. *Polymer* 1986, **27**, 1391
- 8 Gehrke, R., Reikel, C. and Zachmann, H. G. *Polymer* 1989, **30**, 1582
- 9 Geil, P. H. in 'Order in the Amorphous State of Polymers' (Eds S. E. Keinath, R. L. Miller and J. K. Rieke), Plenum, New York, 1987
- 10 Herglotz, H. K. *J. Colloid Interface Sci.* 1980, **75**, 105
- 11 Thompson, A. B. and Woods, D. W. *Nature* 1955, **176**, 78
- 12 de Daubeny, R., Bunn, C. W. and Brown, C. J. *Proc. R. Soc. London, Ser. A* 1954, **226**, 531
- 13 Fischer, E. W. and Fakirov, S. *J. Mater. Sci.* 1976, **11**, 1041
- 14 Hayashi, H., Hamada, F., Suehiro, S., Masaki, N., Ogawa, T. and Miyaji, H. *J. Appl. Cryst.* 1988, **21**, 330
- 15 Wendorff, J. H. and Fischer, E. W. *Kolloid Z. Z. Polym.* 1973, **251**, 884
- 16 Benoit, H., Wu, W., Benmouna, M., Mozer, B., Bauer, B. and Lapp, A. *Macromolecules* 1985, **18**, 986
- 17 Debye, P. and Bueche, A. M. *J. Appl. Phys.* 1949, **20**, 518
- 18 Imai, M., Mori, K., Mizukami, T., Kanaya, T. and Kaji, K. *Polym. Prepr. Jpn* 1989, **38**, 3353
- 19 Gupta, M. R. and Yeh, G. S. Y. *J. Macromol. Sci. Phys.* 1978, **B15**, 119
- 20 Wunderlich, B. 'Macromolecular Physics', Vol. 2, Academic Press, New York, 1976